Simulation methodology for the assessment of the structural safety of concrete tunnel linings based on CFD fire – FE thermo-mechanical analysis: a case study

Simulation methodology for the assessment of the structural safety of concrete tunnel linings based on CFD fire – FE thermo-mechanical analysis: a case study

Patrizia Bernardi[a*], Elena Michelini[a], Alice Sirico[a], Sara Rainieri[a], Carlo Corradi[b]

[a] Department of Engineering and Architecture, University of Parma, P.co Area delle Scienze 181/A, 43124 Parma, Italy

[b] Energy Efficiency Research Srl, P.co Area delle Scienze 181/A, 43124 Parma, Italy

* Corresponding Author: patrizia.bernardi@unipr.it

ABSTRACT

This work aims to provide a comprehensive procedure for the assessment of structural safety of tunnel linings exposed to fire. To this purpose, numerical simulations that model the three fundamental features influencing tunnel fire safety design, namely fire dynamics, thermal behavior and structural response, are performed. Fire development within tunnel is simulated by applying advanced Computational Fluid Dynamics (CFD) techniques under a Fire Safety Engineering (FSE) approach. CFD fire simulation is carried out first, and then the results are transferred into a thermo-mechanical Finite Element (FE) model. A "sequentially coupled thermo-mechanical analysis" is then performed by linking a heat-transfer analysis that provides the temperature distribution within the lining with a refined non-linear mechanical simulation. A proper non-linear constitutive model for concrete subjected to high temperature, able to account the main features governing concrete behavior (i.e. cracking and crushing), is applied to the purpose. Comparisons in terms of structural results obtained by applying this coupled procedure and those obtained through a thermo-mechanical analysis adopting a standard time-dependent fire curve are provided. The importance of considering a refined simulation of the fire scenario is proved: from a structural point of view, significant differences concerning stress distribution and cracking development in the lining are indeed observed. Therefore, the use of a realistic model to describe fire development appears crucial

to understand the behavior of unreinforced concrete linings subjected to fire and to control their possible weaknesses, such as the appearance of cracks.

Keywords: *tunnel lining; fire safety engineering; CFD - FE coupled analysis; concrete constitutive model; FE thermo-mechanical analysis*

Nomenclature

B	parameter that defines the post-failure behavior in compression of concrete
c	rock mass cohesion
D_t	tunnel diameter
$[D]$	total material stiffness matrix
$[D_c]$	concrete stiffness matrix
$[D_{cr1}]$	crack stiffness matrix
E_{ci}	"initial" value of concrete Young modulus, which represents the slope of the initial straight portion of the stress-strain curve that depends on temperature
E_r	Young modulus of the rock mass
H	tunnel depth below the ground surface
L	tunnel length
$f_{c,20\,°C}$	uniaxial compressive strength of concrete at ambient temperature
f_c	concrete uniaxial compressive strength, which depends on temperature
f_{ct}	concrete tensile strength of concrete, which depends on temperature
v_1	crack sliding
w_1	crack width
ε_{c0}	concrete compressive peak strain, which depends on temperature
$\{\varepsilon\}$	total strain vector
$\{\varepsilon_c\}$	concrete strain vector
$\{\varepsilon_{cr1}\}$	crack strain vector
$\{\varepsilon_{th}\}$	thermal strain vector
γ_c	concrete specific weight
γ_r	rock mass specific weight
ϕ	rock mass friction angle
ν_r	rock mass Poisson coefficient
ν_i	"initial" value of concrete Poisson coefficient, which depends on temperature
$\{\sigma\}$	total stress vector
$\{\sigma_c\}$	concrete stress vector
$\{\sigma_{cr}\}$	stress vector in the crack

Other symbols are defined as they appear in the text.

1 Introduction

The safety assessment of tunnels subjected to fire is a fundamental task, since the disaster caused by fire in tunnels may result in the loss of human lives and in considerable economic damages, as demonstrated by the high number of tunnel fires occurred during last decades. For this reason, the scientific community, together with designers, is showing an increasing interest towards the development of more or less sophisticated approaches able to afford this issue, with the aim of mitigating fire hazard in road infrastructures, given the rapid urbanization and the increase in fuel and chemical products shipments [1,2].

The analysis of the behavior of linings during fire plays an important role in the assessment of tunnel safety. Fire design of tunnel linings should be aimed to guarantee the structural integrity at high temperatures and to ensure a sufficient residual capacity to sustain fire effects without collapsing [3–5]. This represents a complicated issue, not only because of the peculiarity of fire development in tunnels, but also because of the complexity of structural element response at high temperatures. Both the fire development and the structural response are influenced by several parameters (among others the geometrical configuration of the tunnel, the interaction with the surrounding rock mass and the consequent confinement action).

As known, the problem involves three main physical aspects: fire development, heat transfer and structural response; each of these aspects can be treated with a different level of complexity and must be properly coupled with the other ones.

In design process, under the so-called “prescriptive approach”, when the focus of investigation is the assessment of the fire safety of the lining, rather than the study of the fire itself, standard fire curves are commonly applied to represent fire development. Following this approach, the fire scenario, which is required as input data for the thermo-mechanical analysis, is represented by a simplified time-dependent relationship. Since Eurocode 2 – Part 1-2 [6] does not provide specific suggestions for tunnel fire loading, different time-temperature curves can be adopted, from the

standard ISO 834, to the Rijkswaterstaat RWS or to the more specific Hydrocarbon modified HCM or RABT/ZTV fire curves [7–9]. ISO 834 curve, which is representative of a cellulosic fire, with a relative slow temperature rise, is largely adopted for structural applications and fire testing on building materials. This curve is also suggested for tunnel design by ITA-AITES Guidelines [8], at least when the expected traffic type is mainly represented by cars and small vans. However, tunnel fires are quite different from cellulosic ones, due to several factors: the high calorific potential of the involved materials (such as vehicle fuels and the vehicles themselves), the confinement of the heat release, as well as the interaction of the ventilation system with the growing fire plume. For these reasons, HCM, RABT/ZTV and RWS fire curves, specifically developed for highly combustible materials, are more often adopted for the assessment of tunnel structural safety, since their use provides results which are sufficiently conservative and always on the safe side [7]. However, regardless of the used curve, this standardized design approach is based on simplified post-flashover scenarios that describe the fire growth under a lumped-parameter zone model. Therefore, the use of these fire curves cannot ensure an accurate description of the real fire scenario in tunnels, because it is very unlikely that a fire grows uniformly over the entire enclosure. Tunnel fire gives raise to complex non-uniform three-dimensional unsteady flows related to smoke and flame spread, which generally result in temperatures higher at the ceiling and lower at the walls. These complex phenomena can be only handled by using Computational Fluid Dynamics (CFD) techniques that can simulate, although with high computational costs, the multi-physic interactions that occur during fire. For this reason, CFD techniques are becoming a common strategy under the Fire Safety Engineering (FSE) approach (among others, e.g., [10–12]), especially when the attention is focused on the evaluation of the prevention, protection and suppression systems of tunnels, as well as on the emergency procedures.

The application of CFD results to structural purposes is still not widespread in design practice. This is mainly due to the difficulties related to the coupling of fire simulation, heat-transfer and structural

response. However, some recent research works, focused on single structural elements or single rooms, have shown the effectiveness of combining CFD and FE techniques (among others, [13–17]). These works apply sophisticated analyses where the coupling between CFD and FE simulations is handled in detail. A distinction can be made between "two-way" [13] or "one-way" [14–17] approaches, depending if the effects of structural analysis on fire development are or not taken into account. However, to the knowledge of the Authors, there is a lack of published works focusing on the application of CFD and NLFEA to the case of tunnel linings, even if these methods can represent an interesting solution for the mitigation of fire hazard in underground structures. The here proposed work wants to be a first attempt in this direction, since it aims to clarify the influence exerted by the refinement degree in the analysis of fire development on the assessment of structural safety of a concrete tunnel lining. To this end, a coupled analysis able to both represent the fire scenario and analyze the thermal and structural behavior of the tunnel lining is presented. A one-way approach is followed, due to the complexity of the examined case-study and to the refinement degree of the FE structural analysis, which is here conceived to take into account ground-lining interaction, as well as non-linear mechanical behavior of concrete. A properly developed constitutive model including cracking, crushing, thermal strains and material degradation with temperature, is used. The adoption of such a complex mechanical model allows to highlight the influence of the fire scenario simulation on stress distribution and cracking development in the lining, since it is able to account for all the main features governing concrete non-linear behavior. Furthermore, it can also provide an estimate of crack width, which represents the most critical design issue when considering unreinforced concrete lining [8].

2 Coupled FDS-FEM method for the structural analysis of a concrete tunnel lining subjected to fire

A fire simulation is carried out through the software Fire Dynamics Simulator FDS [18] by adopting a CFD approach in order to study the development of a real fire scenario. Then, the obtained data are transferred into a FE model realized with the commercial code ABAQUS [19]. A "one way" coupling strategy is followed: according to this procedure, fire simulation is performed before the FE heat transfer and mechanical analyses, without transferring back the structural results of the thermo-mechanical analysis to FDS. The results of fire simulations are used to compute the boundary conditions of the subsequent thermo-mechanical analysis, by means of adiabatic surface temperature (AST). As concerns thermo-mechanical analysis, a "sequentially-coupled thermal stress procedure" is adopted, according to the definition provided in ABAQUS Manual. This means that the stress-displacement solution is dependent on the temperature field, but there is no inverse dependency, i.e. the temperature distribution in the studied element is independent from its structural behavior.

The crucial point of the procedure is the linking of the different models developed to analyze each stage (Fig. 1). CFD and FE models are usually characterized by different spatial discretization and time scales, which make the coupling not a trivial task. For this reason, a proper interpolation of CFD results is required for each time interval. In order to minimize the number of parameters passed from the CFD simulation to the FE one [13,14] adiabatic surface temperature (AST) is used, accordingly to the definition provided in [20,21]. AST is calculated during the CFD simulation and registered through point measurements (by means of a device grid, see Figure 1). The obtained data are stored in an output file with comma separated values (CSV file). AST values are first interpolated through a properly developed MatLab routine in order to match the differences in discretization and time scales between CFD and FE simulations; then, they are passed as input parameters into the FE heat-transfer analysis. For each integration point placed at the lining intrados

surface and at pavement surface of the FE thermal model, input data at each time instant are obtained by linearly interpolating the results registered in the nearest points of the device grid in the CFD model (Fig. 1).

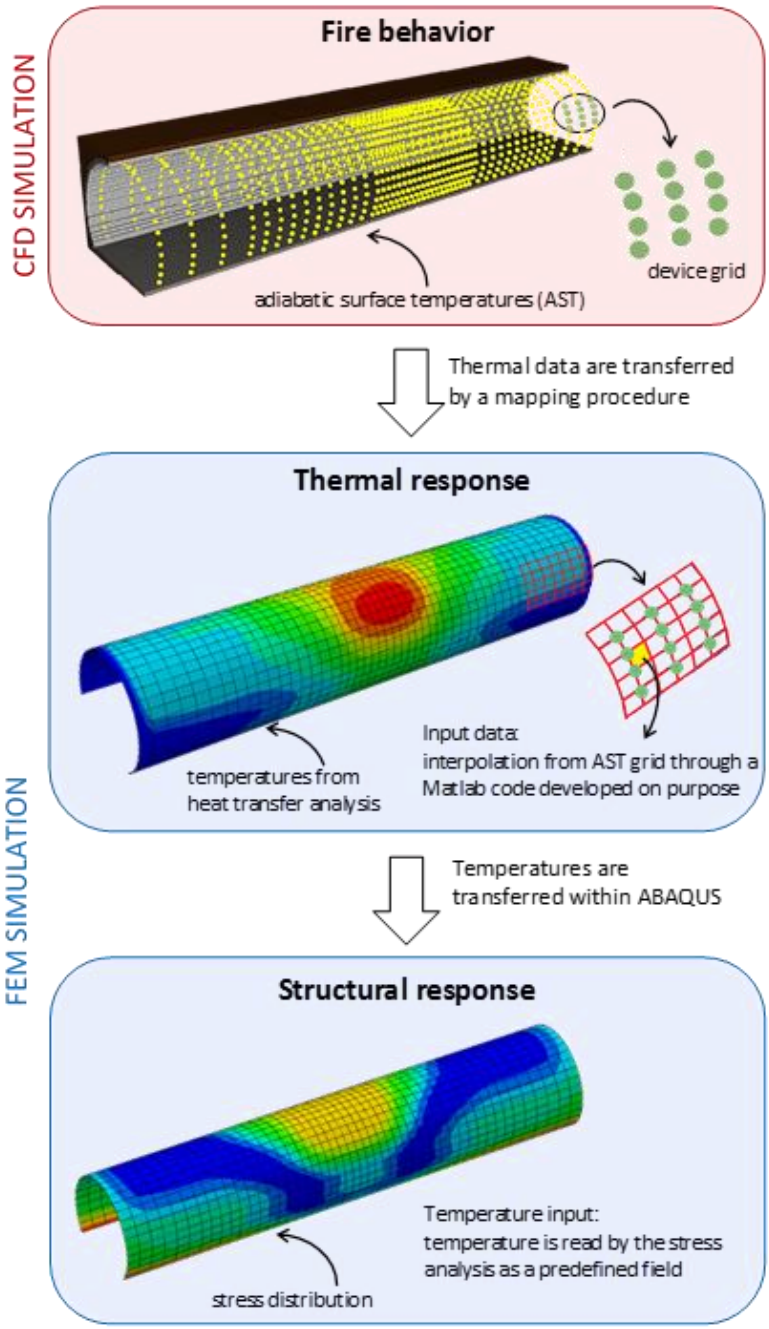

Figure 1 – Procedure for coupling CFD fire simulation to FE thermo-mechanical analysis.

Once the thermal response is obtained, the mechanical analysis is carried out by applying the transient temperature field derived from the thermal simulation as a predefined field. As already mentioned, a so called “sequentially-coupled thermo-mechanical analysis” is carried out; in this way, it is possible to perform first the heat-transfer analysis and subsequently the mechanical one. Since both the heat-transfer and the structural analysis are performed through the FE code ABAQUS, the interaction between the two simulations is internally managed and no further actions are required. Moreover, the same mesh can be adopted for both the heat-transfer analysis and the subsequent structural simulation, by using respectively heat-transfer and stress elements.

2.1 CFD Simulation

CFD analysis is performed within FDS environment [18]. The Navier-Stokes equations are solved using a second-order finite difference numerical scheme with a low-Mach number formulation, while the turbulence modeling is based on the Large Eddy Simulation (LES) approach. With regard to the combustion model, FDS adopts the mixing-limited infinitely fast reaction of “lumped species” – which are reacting scalars that represent mixtures of species – approach. Thermal radiation is computed by solving the radiation transport equation for gray gas using the Finite Volume Method (FVM) on the same grid as the flow and heat transfer solver. Detailed descriptions of the mathematical models used in FDS can be found in [18].

The use of FDS also for multi-disciplinary fire simulations has become a well assessed methodology also for complex systems, although some care must be adopted in both model construction and data processing. In particular, an important issue is related to the parameters that have to be monitored in the fire simulation, since a coupled thermo-mechanical analysis has to be performed. Moreover, in the numerical solution scheme implemented in FDS, special attention must be taken in the selection of the grid cell size. In fact, the size of a single cell of the calculation grid strongly affects the reliability of the simulation outcomes.

2.2 FE thermo-mechanical analysis

2.2.1 Thermal analysis

Thermal analysis, which accounts for all the three mechanisms ruling heat-transfer, namely conduction, convection and radiation, is performed in order to obtain the transient temperature field within concrete lining, rock mass and paving. To this aim, the adiabatic surface temperature provided by FDS is used as boundary conditions in ABAQUS. In this way, the temperature profiles within the element under examination are computed by considering a realistic fire scenario and adopting the same material thermal properties considered for FDS simulation.

For comparison, a thermal analysis based on RWS fire curve is also performed. Among other fire curves available in technical literature, RWS is chosen herein because it better represents the high temperatures developed by large vehicle fires (like trucks/tankers) in an enclosed environment, being specifically derived for tunnel design on the basis of laboratory tests carried out in the Netherlands [22]. In this case, the heat-transfer simulation is performed by applying the prescribed nominal temperature curve uniformly to all the intrados surface of the lining as boundary condition (by considering that heat transfer from the heated gas to the concrete surface is governed by radiation and convection).

2.2.2 FE mechanical analysis

Mechanical analysis is developed in two main steps, corresponding to the application of the in-situ state of stress deriving from the excavation and lining installation phases, and to the simulation of the fire load. Since the focus of this work is the evaluation of tunnel behavior under fire conditions, the simulation of tunnel realization phases is herein simplified, i.e. it refers directly to the final equilibrium condition between the support system and the surrounding ground, typical of a service-life condition. However, a more refined simulation could be performed, as presented by some of the

Authors in [23], by adopting a step-by-step procedure able to simulate the gradual tunnel excavation and subsequent lining installation.

Once the service loads are applied, the transient temperature field derived from the thermal simulation is read automatically by the structural analysis, as a predefined condition. The aim is to obtain the stress-strain evolution in the lining and in the ground during fire exposure. To this end, it is necessary to include in the model both geometric non-linearity and reliable constitutive relationships for the involved materials, able to account for thermal induced effects (i.e. thermal strains in the materials, together with the decay of their mechanical properties).

Regarding ground behavior, the classic Mohr-Coulomb elasto-plastic constitutive law is used. Since during fire the ground surrounding the tunnel usually remains at ambient temperature (20° C) thanks to the good insulation properties of concrete, it is not necessary in this case to simulate the degradation of mechanical properties, as well as the appearance of thermal strains.

On the contrary, it is mandatory to take into account thermal effects on concrete. Moreover, in the analysis of the behavior of tunnel linings it is particularly important to adopt material models able to account for the effects of crushing and cracking. Concrete linings may present high compressive stresses during fire, due to the stress relaxation near the heated surface and to the deformation constraint in the circumferential direction exerted by the cold extrados and the ground; hence, the importance of considering crushing and dilation in compression. When analyzing shotcrete and unreinforced concrete linings, cracking is a variable of paramount importance, since the most critical design issue is usually represented by crack width [24–26].

The non-linear response of concrete is managed through a constitutive model (named “2D-PARC FIRE”) developed by the first three Authors, based on an existing smeared, fixed crack formulation for reinforced concrete elements at ambient temperature, named 2D –PARC [27]. The model enables a refined crack modeling – being able to represent in a realistic way all the resistant mechanisms that take place after crack formation – as well as a reliable estimate of crack width

(among others [28–30]). Moreover, concrete behavior under different loading combinations, also in the post-crushing region, is accurately described through the adoption of an isotropic non-linear elastic formulation [29]. This constitutive model, is implemented as a User MATerial (UMAT) subroutine within the adopted FE code, allowing not only an effective crack pattern analysis but also a good numerical stability when compared with other constitutive relations for concrete available in ABAQUS [31].

2.2.2.1 Concrete constitutive model: 2D-PARC FIRE

The simulation of lining behavior under fire conditions has required a proper extension of 2D-PARC model [27,29] – named 2D-PARC FIRE – in order to include in the algorithm additional features, like thermal strains and the degradation of concrete properties due to high temperatures. Furthermore, crushing and dilatation are modified in 2D-PARC FIRE, by calibrating the parameters governing the post-peak behavior of concrete.

In order to take into account thermal strains, the basic equilibrium and compatibility equations of 2D-PARC model have been reformulated, according to [32]. The followed procedure is herein briefly recalled for the considered case of an unreinforced concrete lining.

In the uncracked stage, the stress field in concrete is derived from the corresponding mechanical strain, suitably corrected by including the contribution of the free thermal strain $\{\varepsilon_{th}\}$, which is considered stress independent and isotropic. The shear component of this free thermal strain vector is assumed equal to zero, while the other terms are evaluated for each integration point as a function of the temperature *T*, obtained from the heat-transfer analysis, by following the relation suggested by Eurocode 2 – Part 1-2 [6] in case of siliceous aggregates in the concrete admixture:

$$\begin{cases} \varepsilon_{th}(T) = -1.8\cdot10^{-4} + 9\cdot10^{-6}T + 2.3\cdot10^{-11}T^3 & 20°C \le T \le 700°C \\ \varepsilon_{th}(T) = 14\cdot10^{-3} & 700°C \le T \le 1200°C \end{cases} \quad (1)$$

All the involved concrete mechanical parameters within the algorithm are introduced as temperature-dependent variables, so to take into account the loss of strength and stiffness undergone

by the material during heating, according to the laws proposed in Eurocode 2 – Part 1-2 [6]. More in detail, the concrete stiffness matrix [D_c] is updated during the analysis in order to describe concrete behavior under a general biaxial state of stress in presence of high temperature. On the basis of the current state of stress, the input parameters required by the model (E_{ci}, ν_i, f_{ct}, f_c, ε_{c0}, B) are properly updated (by following a non-linear elastic formulation, see [29]), while the degradation of concrete mechanical properties due to fire is taken into account by inserting the dependency of these input data on temperature T. In this way, the failure envelope retains the same shape as at ambient temperature, while its reduction due to high temperatures is automatically computed on the basis of the input parameters.

When the current stress state reaches the adopted failure envelope in the region of prevailing tension, the transition to the cracked stage takes place. A single fixed crack model based on strain decomposition is applied. The cracked stage is assumed to be characterized by a fully developed crack pattern (corresponding to the stabilized cracking stage), by considering a constant value of crack spacing. In case of unreinforced concrete, this value is set equal to $3d_{max}$, where d_{max} represents the maximum aggregate size, according to the suggestions provided by Bažant & Oh [33].

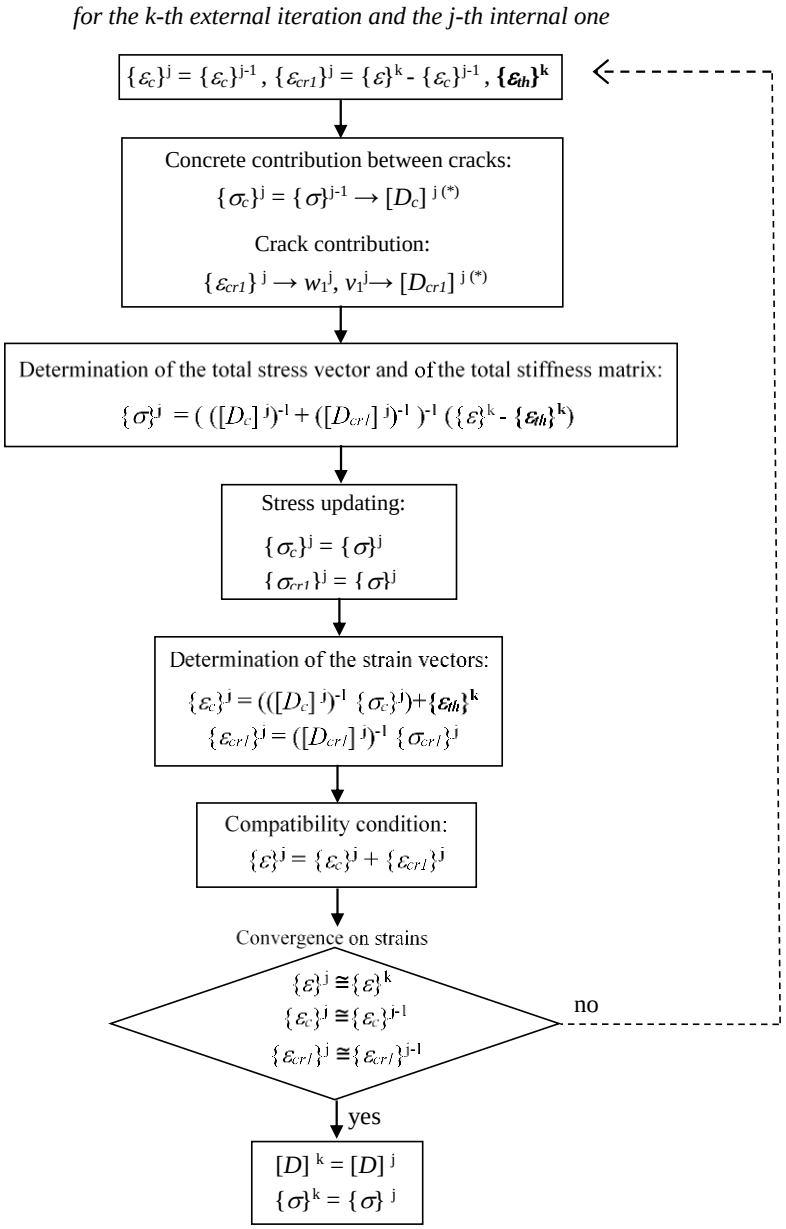

k: iteration performed by ABAQUS to try to bring the internal and external forces into balance

j: iteration performed by 2D-PARC-FIRE to try to achieve convergence on strains

(*) Matrix $[D_c]$ and matrix $[D_{cr1}]$ are computed by considering the dependance of the main mechanical parameters from temperature

Figure 2 – Flow chart of the procedure adopted in the cracked stage in 2D-PARC FIRE for each FE integration point.

In the adopted procedure, the total strain $\{\varepsilon\}$ is so subdivided into two components, namely $\{\varepsilon_c\}$, related to concrete between cracks, and $\{\varepsilon_{cr1}\}$ including all the mechanisms taking place in the fracture zone. To determine the current values of these two components an iterative procedure is

performed within the Users' Subroutine, as shortly reported in Figure 2. The aim of this internal cycle of iterations is to determine the total stiffness matrix [D] and stress vector $\{\sigma\}$ to be passed to ABAQUS for each iteration within a given loading increment.

It can be observed from Figure 2 that the expression of the total stress vector $\{\sigma\}$ is function of the stiffness matrix of concrete between two adjacent cracks [D_c], and of the crack stiffness matrix [D_{cr1}]. This latter incorporates all the resistant mechanisms developing across crack surfaces (i.e. aggregate bridging and interlock), determined on the basis of the current values of crack width w_1 and sliding v_1. The mechanical laws adopted for the description of aggregate bridging and interlock, which are related to fracture energy G_f, have the same formal expressions as for concrete at ambient temperature (see [27]). However, in case of fire, concrete properties are temperature-dependent variables, thus the mechanical laws are consequently scaled in case of high temperature. This seems to be a reasonable choice, since, although there are in literature many works that investigate the dependency of G_f on temperature, a general agreement has not been found yet. Moreover, most of these studies present results that are often qualitative and not quantitative [34], so the dependency of aggregate bridging and interlock laws on temperature is herein related only to the degradation of their input data.

Finally, it should be mentioned that, in case of tunnels, transient creep strain (i.e., the additional strain that develops irrecoverably during first-time heating of concrete under load, compared to concrete loaded at elevated temperature [35]), should be also taken into account in the analysis. In 2D-PARC FIRE, its effect is implicitly included in the model through the adoption of the uniaxial compressive stress-strain relation (with non-linear descending branch) for concrete at high temperatures suggested by Eurocode 2 – Part 1-2 [6]. This relation implicitly takes into account the load induced thermal strains (LITS), by "artificially" increasing the strain parameters (which are required for the definition of the stress-strain curve in presence of fire) with increasing temperatures, beyond their actual values (as also suggested in [36,37]). In this way, the tangent

modulus is decreased by a fixed amount at each temperature increment, allowing the development of an equivalent transient strain at constant load levels with increasing temperature [38]. Even if this implicit model has some limitations, especially during the cooling phase, it is widely used in numerical modelling, since it leads to quite satisfactory results in the most of structural applications.

3 Case study

The above described procedure is herein applied to the analysis of a deep circular road tunnel, excavated in a poor quality rock mass (which can be assimilated to schist). The tunnel is supported by a single shell sprayed concrete ring of class C45/55, with a thickness of 600 mm and an inner radius of 6.75 m (Fig. 3). The tunnel is 70 m long and is located about 80 m below the ground surface. It is considered to be subjected to a natural isotropic stress state, so assuming the coefficient of lateral earth pressure at rest K_0 – relating horizontal (σ'_h) to vertical (σ'_v) effective stresses in the undisturbed condition – equal to 1 ($K_0 = \sigma'_h / \sigma'_v$).

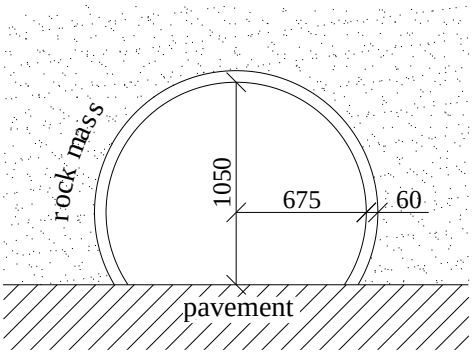

Figure 3 – Geometry of the tunnel cross-section assumed as case-study (dimensions in cm).

Table 1 summarises the main material mechanical properties adopted in the analysis. Concrete mechanical properties at ambient temperature required for the modelling (i.e. $E_{c,20°C}$, $f_{ct,20°C}$, $\nu_{,20°C}$ and $\varepsilon_{c0,20°C}$) are derived from the compressive strength value $f_{c,20°C}$ at 20°C, according to Eurocode 2

– Part 1-1 [39], while the degradation of these properties with temperature is evaluated according to Eurocode 2 – Part 1-2 [6].

In order to take into account material degradation in compression due to high temperature, the non-linear elastic model used in 2D-PARC FIRE for the description of concrete behavior is calibrated on the basis of the uniaxial curve proposed in Eurocode 2 – Part 1-2 [6], which is reported for the examined case in Figure 4. In this way, E_{ci}, f_c, ε_{c0}, B are properly defined. From the same Figure, it can be observed that the stress-strain relation evaluated according to EC2 – Part 1-2 [6] for concrete at 20°C (continuous line) is different from that suggested by EC2 – Part 1-1 [39] for concrete at ambient temperature (dotted line).

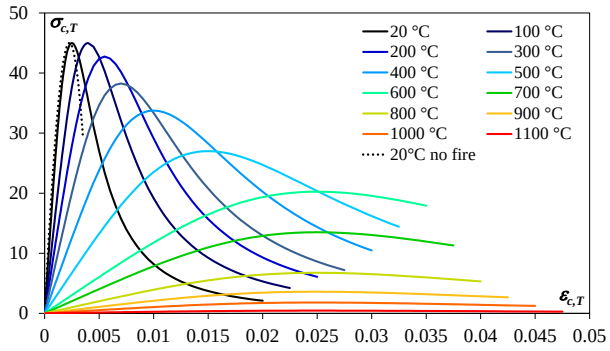

Figure 4 – Stress-strain relation for concrete under uniaxial compression at elevated temperatures.

The value of concrete tensile strength, f_{ct}, is kept constant until 100°C and then a linear decrease is adopted, resulting in a final value equal to zero at 600°C, according to Eurocode 2 – Part 1-2 [6]. Concrete thermal properties are set once again in agreement with Eurocode 2 – Part 1-2 [6].

Specific heat c_c is calculated referring to a moisture content of 1.5% by weight, as follows:

$$c_c = \begin{cases} 900 & 20°C \le T \le 100°C \\ 1470 & 100°C \le T \le 115°C \\ 1470 - 470/85 \cdot (T - 115) & 115°C \le T \le 200°C \\ 1100 + (T - 400)/2 & 200°C \le T \le 400°C \\ 1100 & T \ge 400°C \end{cases} \quad (2)$$

while thermal conductivity λ_c is determined with reference to the lower limit expression, since the structure is herein represented by an unreinforced concrete ring:

$$\lambda_c = 1.36 - 0.136\frac{T}{1000} + 0.0057\left(\frac{T}{100}\right)^2 . \quad (3)$$

As concerns emissivity, the value 0.9 is adopted.

For the surrounding ground and the road paving, constant average values of thermal properties taken from technical literature are assumed, as reported in Table 2. As already mentioned, in this case, it is not necessary to consider the evolution of mechanical properties with temperature, due to the good insulation properties of concrete; hence, the values specified in Table 1 for the rock mass are used for all the duration of fire exposure.

Table 1 – Mechanical properties assumed for the rock mass and for the concrete lining.

Rock mass					***Concrete lining***	
γ_r **[kN/m³]**	E_r **[MPa]**	ν_r	ϕ **[°]**	**c [MPa]**	γ_c **[kN/m³]**	$f_{c,20°C}$ **[MPa]**
25	1900	0.25	44	0.20	24	45

Table 2 – Thermal properties assumed for the rock mass and the pavement.

Rock mass			***Pavement***		
Specific heat [kJ/kgK]	**Thermal conductivity [W/mK]**	**Emissivity**	**Specific heat [kJ/kgK]**	**Thermal conductivity [W/mK]**	**Emissivity**
1.3	3.5	0.9	1	2.06	0.9

The fire of a heavy goods vehicle is assumed as fire scenario. The Rate of Heat Release (RHR) curve (Fig. 5) is determined on the basis of large-scale fire tests for road tunnels carried out in Spain at TST (Tunnel Safety Testing) [22]. The test involved a typical truck, with volume equal to 10.2 m length x 2.40 m width x 4.50 m height, fully loaded with 48 plastic pallets (20%) and 180 wooden pallets (80%). The fire source was ignited by 2 trays, with each tray containing about 1 liter of gasoline.

For the considered case-study, the fire source is placed at mid-length of the tunnel on the fast lane, so being in an asymmetrical position with respect to the transversal cross section (Fig. 6a).

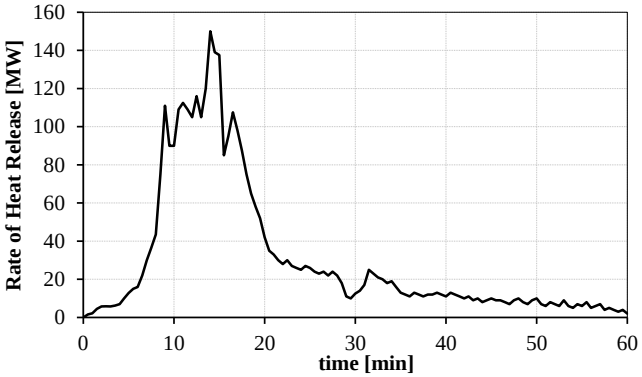

Figure 5 – Rate of Heat Release (RHR) curve of a fire involving a heavy goods vehicle in agreement with large-scale fire tests carried out at TST [22].

3.1 FDS model for fire simulation

For the definition of FDS model, the natural curve is derived by considering a fire scenario based on the RHR curve given in Figure 5 (derived from [22]) that is distributed over the external surface of the burning object by adopting a time dependent heat release rate density boundary condition (HRRPUA: Heat Release Rate Per Unit Area), considering a fire duration of 3600 s. The boundary condition is applied to the top and sides of the solid system used to model the heavy goods vehicle, while the bottom surface is assumed inert. Moreover, the surrounding environment is modeled in detail, in order to take into account the heat flux exchanged with the concrete lining, the paving and part of the rock mass (Fig. 6a).

Within FDS environment, the curved walls of the lining are modelled as a sequence of individual "blocks" and therefore the degree of approximation of the real geometry depends on the mesh resolution. A mesh sensitivity analysis was first performed, and the grid size for the simulations was determined requiring that mesh independent results could be obtained.

The Heskestads correlation [40] is used to estimate the minimum spatial resolution required, according to the heat release rate density and the size of the burning area.

The mesh that assures a correct description of the fire scenario has to be based on a cell size lower than the characteristic dimension of the phenomenon, usually defined as the characteristic fire diameter (D*), i.e., the smaller the characteristic fire diameter, the smaller the cell size should be in order to adequately resolve the fluid flow and fire dynamics.

The characteristic fire diameter (D*) is given by the following relationship derived by the Heskestads's [40] approach to the fire plume [41]:

$$D^* = \left(\frac{\dot{Q}}{\rho_\infty c_p T_\infty \sqrt{g}} \right)^{2/5}, \tag{4}$$

where $\dot{Q}$ is the fire size (kW), $\rho_\infty c_p T_\infty$ is the ambient internal energy per unit volume and g the gravity. The grid size has been selected significantly lower than D* in the portion of the mesh close to the burning object.

To limit calculation time, the model is divided into several grids with different refinement, for a total number of cells equal to 770.000. The grid size that was verified as satisfactory for guaranteeing independent results for the central region of the tunnel, where the fire scenario is located, is characterized by a cell size of 0.2m x 0.2m x 0.2m, in agreement with the recommendations of [42].

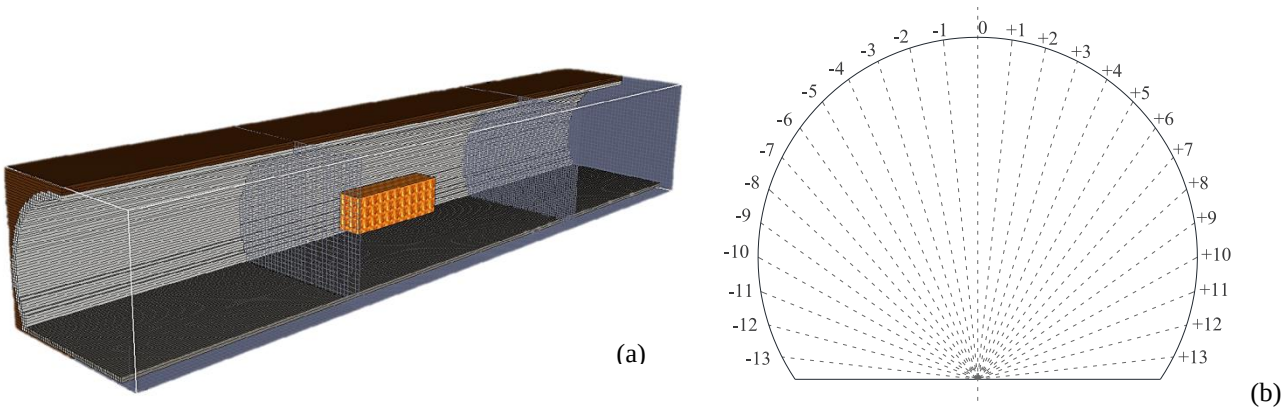

Figure 6 – (a) Geometric domain and grid definition for CFD analysis; (b) devices location in the tunnel transverse cross section.

The heat diffusion into the solid domains (lining, surrounding ground and paving) is described in FDS through a one-dimensional (1D) heat conduction approach. An “open vent condition”, which represents a passive opening to the outside (by default, it is assumed that ambient conditions exist beyond the “open vent”), is attributed to both the entrance and the exit of the tunnel, since in the present case study the effect of mechanical ventilation of the tunnel compartment is not considered. The CFD simulation is tuned to extract both the gas temperature inside the tunnel (in the hot layer in the region close to the burner) and the adiabatic surface temperature of the concrete lining. The gas temperature is used to describe the temperature-time curve associated to the given fire scenario in the specific tunnel environment under test and to compare it to the standard RWS and ISO834 curves, while the adiabatic surface temperature is used as input data of the thermo-mechanical simulation. To this end, thermocouple devices are used to monitor the gas temperature inside the tunnel, while AST values are registered through measurement points. The devices are placed at a mutual distance of about 1 meter over the arc length, according to the scheme reported in Figure 6b. This scheme is repeated in different sections along the tunnel length, resulting in a total number of 1269 devices.

3.2 FE model for thermo-mechanical analysis

The FE model includes the tunnel and a significant portion of the surrounding ground, so to consider the ground-lining interaction (Fig. 7). The extent of the FE mesh in the transverse direction is chosen so as to reach steady-state conditions and to eliminate any influence of the outer boundaries [43,44]. The same extent (approximately equal to 6 times the tunnel diameter D_t) is also considered in the vertical direction, below tunnel axis (Fig. 7a). In order to correctly apply the three-dimensional asymmetric temperature distribution obtained from CFD fire simulation, the whole lining cross section is included in the model (Fig. 7b).

It is worth noticing that, since the thermo-mechanical analysis is "sequentially-coupled" and the coupling between the two simulations is internally managed by ABAQUS, the finite element discretization is kept constant, while the element type changes; i.e. thermal and structural elements are required for thermal and mechanical analysis, respectively.

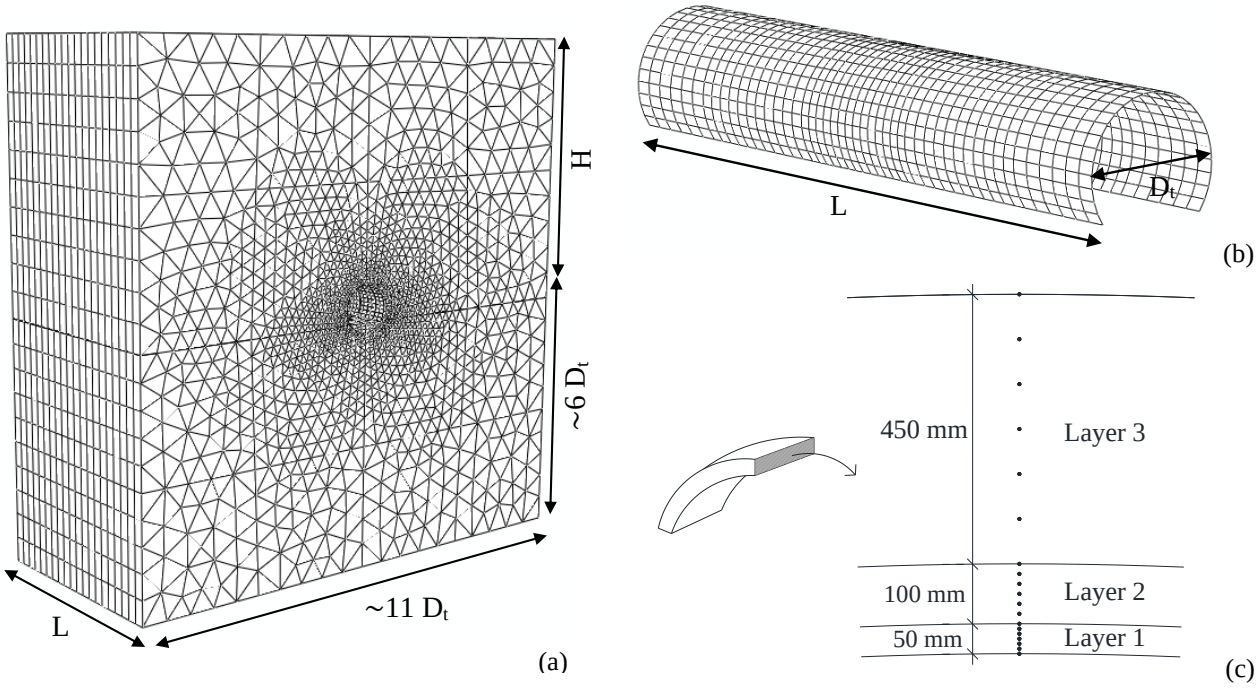

Figure 7 – (a) 3D FE model; (b) detail of concrete lining discretization through shell elements (c) integration points across the thickness of shell elements.

The rock mass and the paving are modeled through prismatic elements (Fig. 7a), while concrete lining through 4-node shell elements (Fig. 7b). These last elements are connected to the ground by means of surface-based ties placed on the outer perimeter of the opening. An offset is assigned to the shell middle plane, so to correctly represent the lining thickness and avoid element interpenetration. A reduced integration technique – with one Gauss point – is adopted in the element plane, while 19 Simpson integration points are considered throughout the thickness (Fig. 7c). The use of a high number of integration points within lining thickness is mandatory when considering fire load, in order to correctly catch the temperature distribution within the concrete ring and the

related hoop stresses. Near lining intrados, where the maximum temperature and stress gradients are expected, integration points are thickened, by subdividing each shell element (representing concrete lining) into several layers with decreasing thickness towards the bore side (Fig. 7c).
The mesh is refined also along tunnel axis in those regions where higher stress and temperature gradients are expected, on the basis of the results of CFD fire simulation (Fig. 7b).

4 Results and discussion

This Section discusses the differences in terms of structural response, when performing a CFD simulation of fire development, rather than adopting a standard time-dependent fire curve (in this case RWS curve) for the assessment of tunnel lining fire safety. To this end, the results of fire simulation (obtained through CFD techniques), as well as that related to the thermal and mechanical response (obtained through FE modelling), are investigated in detail.

4.1 Results of fire scenario modelling

The maximum temperature of the exposed surface resulting from CFD simulation is reported in Figure 8. The peak of heating at lining intrados occurs after 910 s (Fig. 8d), reaching a maximum temperature of 1239°C. Figure 9 reports CFD results also in terms of smoke propagation. As can be seen, in the absence of a ventilation system, the smoke plume propagates immediately above the burning truck, while with the passing of time, a stratified smoke layer forms near the ceiling, both in front and behind the truck. These results can be useful for the design of tunnel ventilation, which however requires more in deep research, outside from the scope of this work.

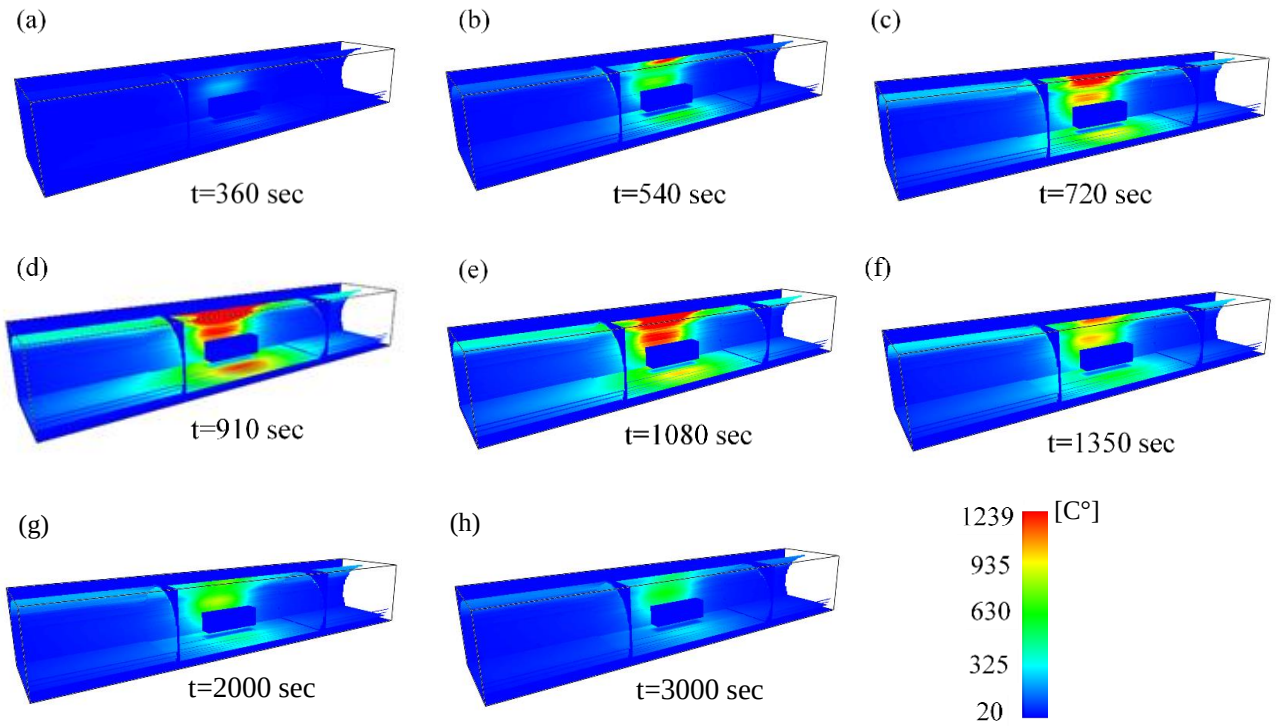

Figure 8 – Wall temperature distribution after:

a) 360 sec; b) 540 sec; c) 720 sec; d) 910 sec; e) 1080 sec; f) 1350 sec; g) 2000 sec; h) 3000 sec.

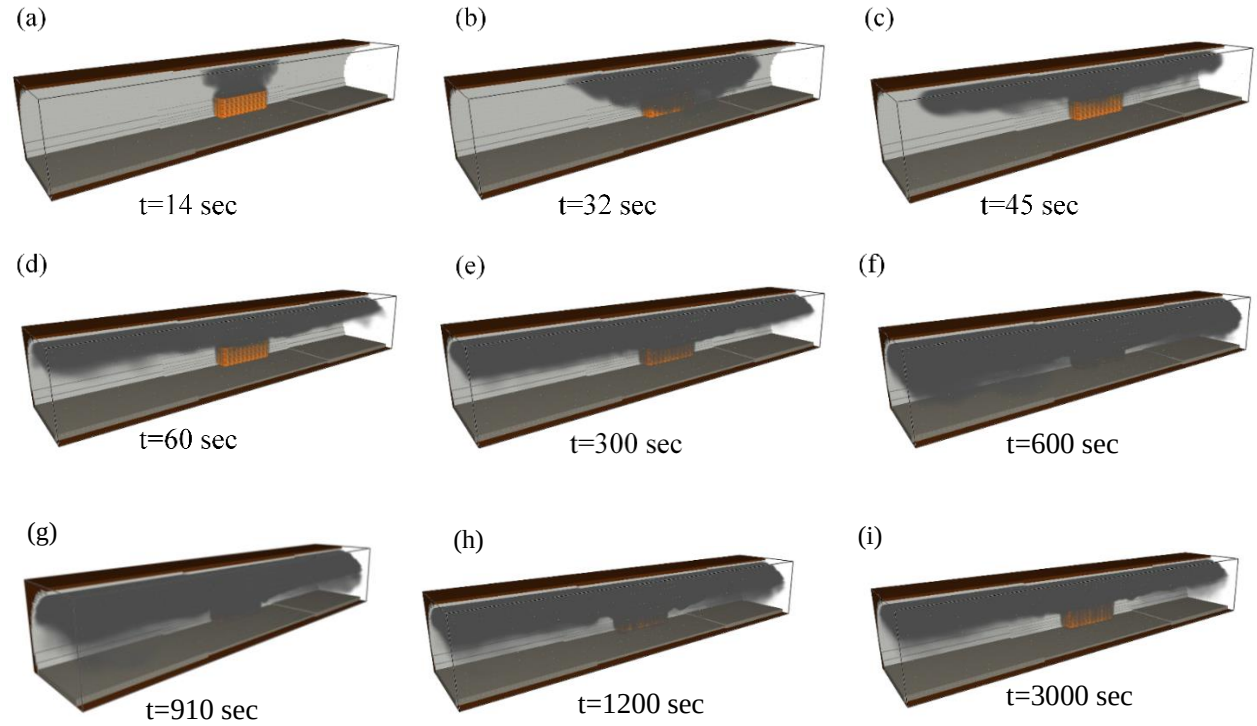

Figure 9 – Smoke propagation after:

a) 14 sec; b) 32 sec; c) 45 sec; d) 60 sec; e) 300 sec; f) 600 sec; g) 910 sec h) 1200 sec; i) 3000 sec.

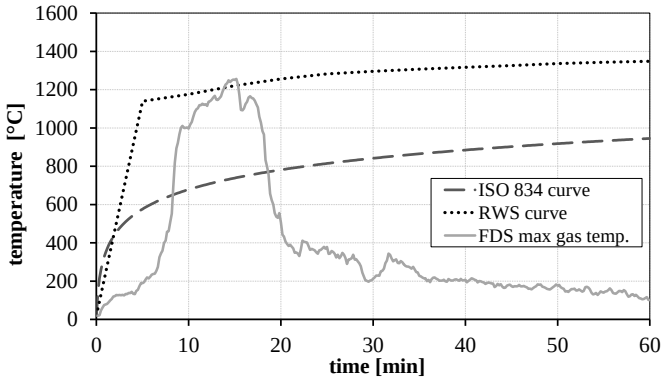

Figure 10 – Comparisons between the standard fire curves (ISO 834 and RWS) and the temperature registered by the thermocouple device (placed at the point of maximum heating) during fire.

The maximum gas temperature due to the considered fire scenario, as registered by the thermocouple devices, is compared in Figure 10 to the standard fire curves ISO 834 and RWS. The data clearly show that the use of these standard fire curves cannot accurately model the considered fire scenario, since the crucial phenomena that occur in the fire compartment are not properly taken into account. First of all, it can be observed that the fire growth stage behavior described by FDS is substantially different from the standard approach. The difference between standard curves and the results of FDS in the first stage can be explained by thinking to the conceptual difference between them. ISO 834 and RWS are nominal fire curves that do not account for the initial phase of ignition and growth of development of fire (see for instance [45]). These standard curves focus on post-flashover phase, since only this stage is important for the fire safety design of buildings. On the other hand, the results of FDS are strictly related to the Rate of Heat Release curve, reported in Figure 5. This curve represents a real fire, based on TST experiment [22], hence, it accounts not only for the post-flashover but also for the pre-flashover phase. With reference to Figure 10, it is worth noticing that the peak gas temperature resulting from CFD simulation is in agreement to the RWS expectation, while for this case ISO 834 represents an inappropriate approach that could lead to unsafe results within the simulation time interval approximately ranging between 10 and 20 minutes.

4.2 Results of thermal simulation

Temperature profiles across lining thickness as obtained from thermal analysis vary in both the length and the transverse perimeter of tunnel, for each time interval, according to the spatial distribution of adiabatic temperatures provided by FDS. As can be expected, higher temperatures are obtained at the ceiling exactly above the truck, while lower values are registered at benches. Moreover, temperatures gradually drop moving away from the burning truck along tunnel length and across lining thickness.

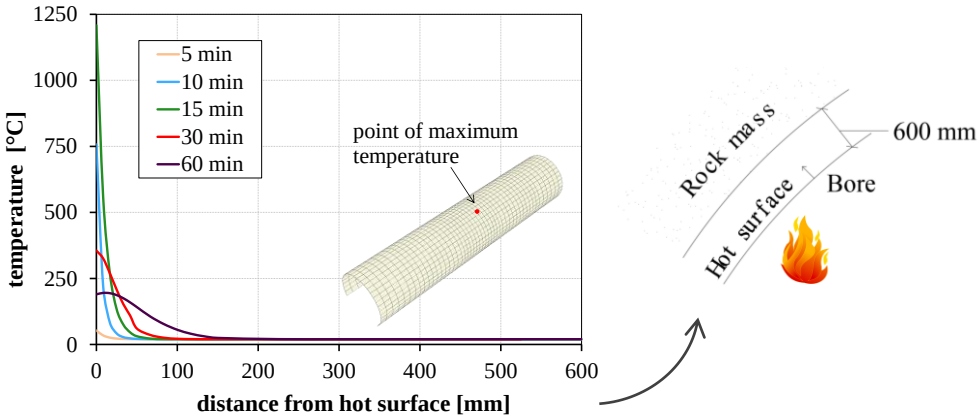

Figure 11 – Temperature distribution across concrete lining thickness referring to the maximum heated point, placed approximately above the fire source, by using as input data the results of CFD fire modeling.

The non-linear distribution of temperatures within lining thickness, relative to the point of maximum heating, is reported in Figure 11 for different fire instants (5 min, 10 min, 15 min, 30 min, 45 min, 60 min).

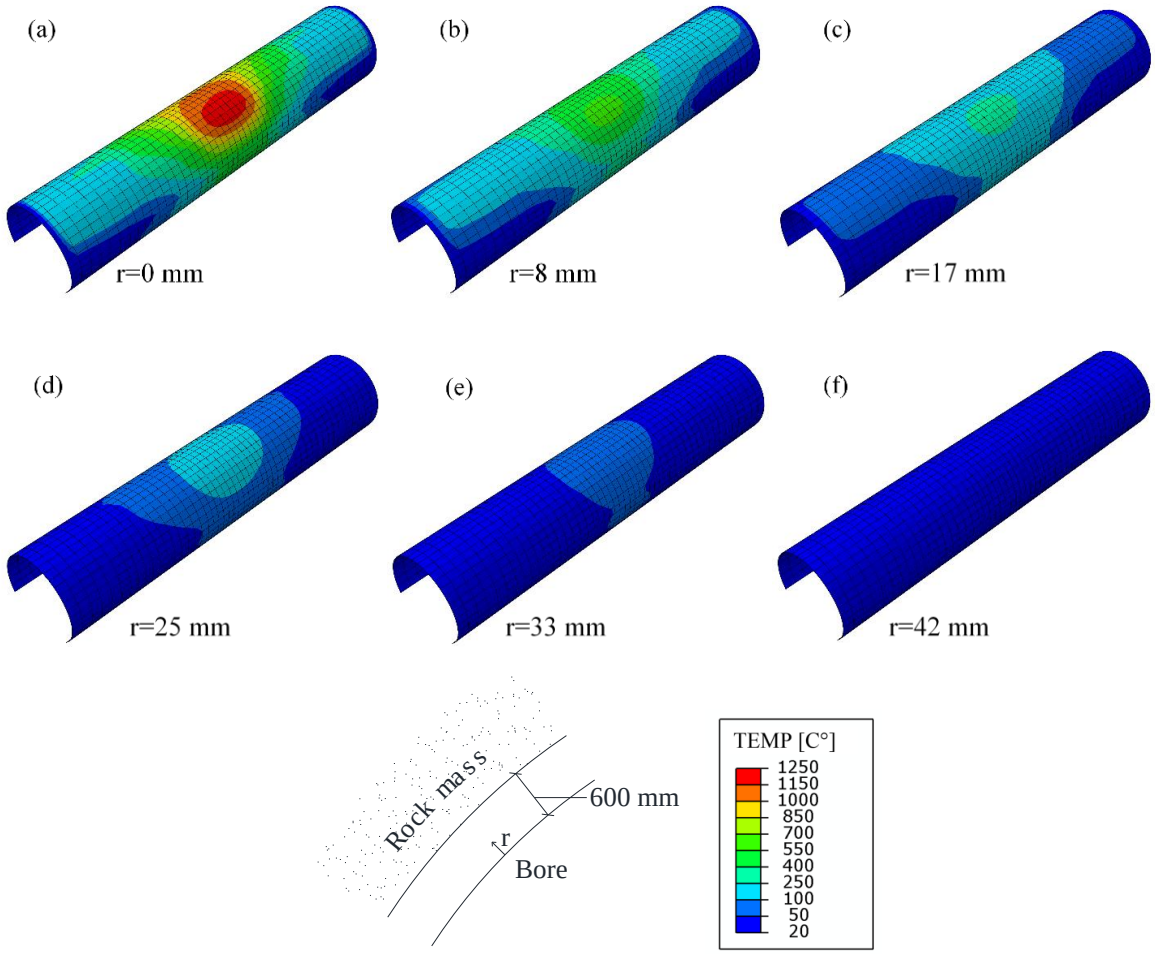

Figure 12 – Temperature distribution after 910 sec of simulation within concrete lining at:

a) 0 mm (intrados surface); b) 8 mm; c) 17 mm; d) 25 mm; e) 33 mm f) 42 mm from lining intrados.

Figure 12 reports the contours relative to the time instant corresponding to the peak of RHR curve (910 s, i.e. about 15 min, when the highest temperature is reached, see Figure 10), for different integration points within concrete lining thickness. At this instant, only about the first 50 mm of the lining (starting from the heated surface) are subjected to temperature increase, thanks to the good insulation properties of concrete. For this reason, the contours relative to the other integration points (placed in the cooler region towards the ground boundary) are omitted. For sake of clarity, all finite elements representing the paving and the rock mass surrounding the lining are switched off from Figure 12.

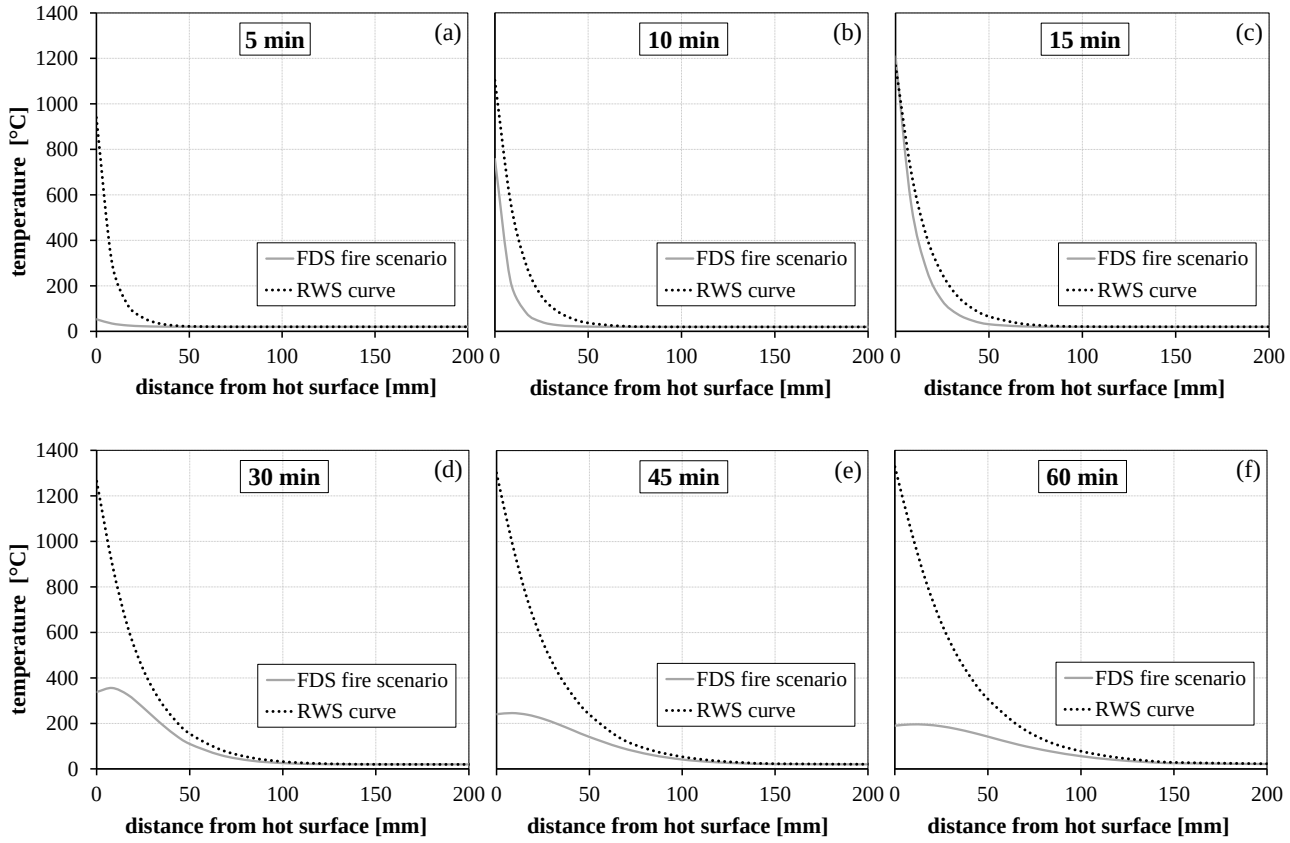

Figure 13 – Comparisons between thermal analysis results obtained by using as input data the results of CFD fire modeling (with reference to the maximum heated point) and those obtained by uniformly applying the RWS curve, after: a) 5 min, b) 10 min, c) 15 min, d) 30 min, e) 45 min, f) 60 min.

In order to highlight the difference between a real fire and a nominal fire scenario, the above described results are compared in Figure 13 to those obtained by uniformly applying RWS fire curve as a boundary condition on the inner surface of the lining (i.e. as input parameter of the thermal simulation). For sake of clarity, the results are reported in Figure 13 only for the first 200 mm of lining thickness starting from its intrados, since the outer zone (nearer to the rock mass) remains at the initial ambient temperature (20°C). These results refer to the maximum heated point when the adiabatic surface temperatures derived from CFD model are applied as boundary condition, while when RWS curve is considered, the obtained temperatures across lining thickness are the same along the whole perimeter and length of tunnel lining.

As can be seen, RWS curve is more severe with respect to FDS fire scenario, above all in the first minutes and during the second half of the simulation, when the difference among the reached

temperature values is more pronounced, since the cooling stage is neglected by RWS curve. It can be also noticed that the temperature profiles in the lining are very similar to each other for the first 15 minutes of fire. These results reflect the differences already observed between RWS fire curve and the fire scenario obtained through FDS (Fig. 10). This confirms that the application of RWS curve produces conservative results in terms of temperatures across lining thickness.

4.3 Results of mechanical simulation

The hoop stresses within lining thickness deriving from the thermo-mechanical analysis that employs as input parameters the adiabatic surface temperatures provided by FDS are reported in Figure 14a. Numerical results, which are relative to the maximum heated point of the lining surface, are referred to the first 15 minutes of fire duration until the reaching of the peak of RHR curve (namely 5 min, 10 min and 15 min).

The stress field shows a typical bell-shaped distribution, which is related to the combined effect of the marked decay experienced by concrete mechanical properties at high temperature – with the consequent stress relaxation near the hot intrados – and of the deformation constraint in the circumferential direction, exerted by the colder extrados. Within the considered time interval, increasing durations of fire exposure determine a shift of the peak stress along lining thickness, from the hotter layers closer to the heated surface to the colder and farther ones. This translation is attributable to the progressive warming of the concrete ring; the increasing temperature acting on the exposed surface causes indeed the heat diffusion in the adjacent layers, with a consequent degradation of material properties. Thus, hoop stresses are redistributed to the reduced, undamaged area. Considering the maximum heated point, the circumferential confinement is not reduced by the appearance of longitudinal cracks at the colder parts of the concrete lining; for this reason, the maximum achieved hoop stress value remains almost the same. This is confirmed by longitudinal stress distribution within lining reported in Fig. 14b.

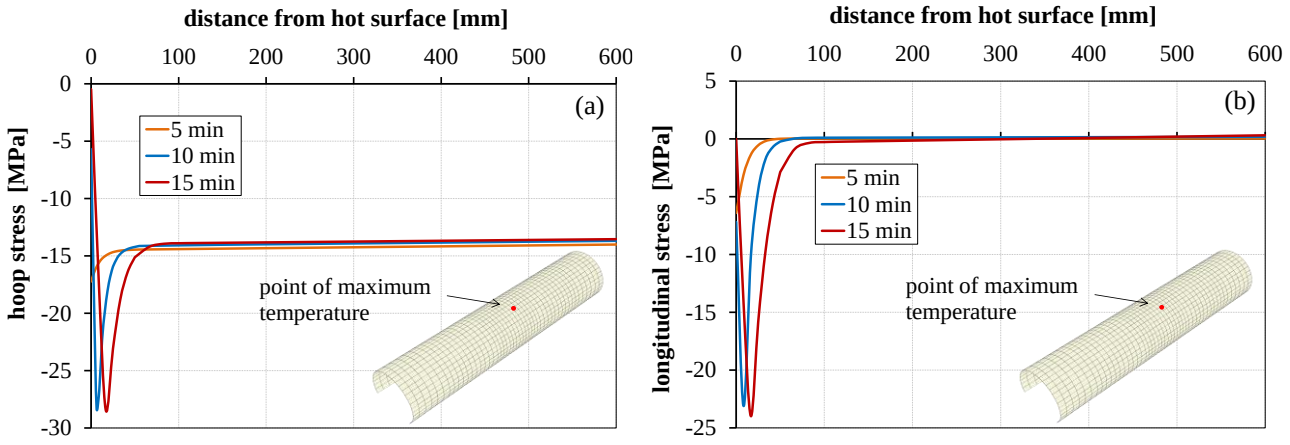

Figure 14 – (a) Hoop and (b) longitudinal stress distribution across concrete lining thickness by exploiting CFD fire modeling and referring to the maximum heated point of the lining.

Hoop stress contours relative to the time instant corresponding to the peak of RHR curve are reported in Figure 15, for different integration points within the thickness of shell elements representing the concrete lining. Similarly to section 4.2, only the results relative to about the first 50 mm of lining near the heated surface are reported in the contours, since the outer zone of the concrete ring (near the ground) is not influenced by fire. As can be seen, a three-dimensional asymmetric stress distribution is obtained. In the intrados surface, hoop stresses become almost equal to zero at the ceiling above the position of the track. Consequently, a stress redistribution can be observed at benches, inside lining thickness, and along the tunnel length, when moving away from the track. The hoop stresses deriving from the thermal simulation that applies RWS curve are reported for comparison in Figure 16. As can be seen, the more pronounced differences are registered at the beginning of fire exposure (5 min), when RWS fire curve shows a faster temperature rise with respect to FDS fire modeling (Fig. 13a). For this reason, in the first fire instants, greater thickness of concrete lining is subjected to the fire-induced damage when considering the RWS curve. This causes a redistribution of stresses within the undamaged colder part of the concrete ring and a consequent translation of the peak of the hoop stress curve. As already observed for thermal results (Fig. 13c), the stress fields in the lining are instead close to each other near the peak of RHR curve (i.e. after 15 min of fire duration).

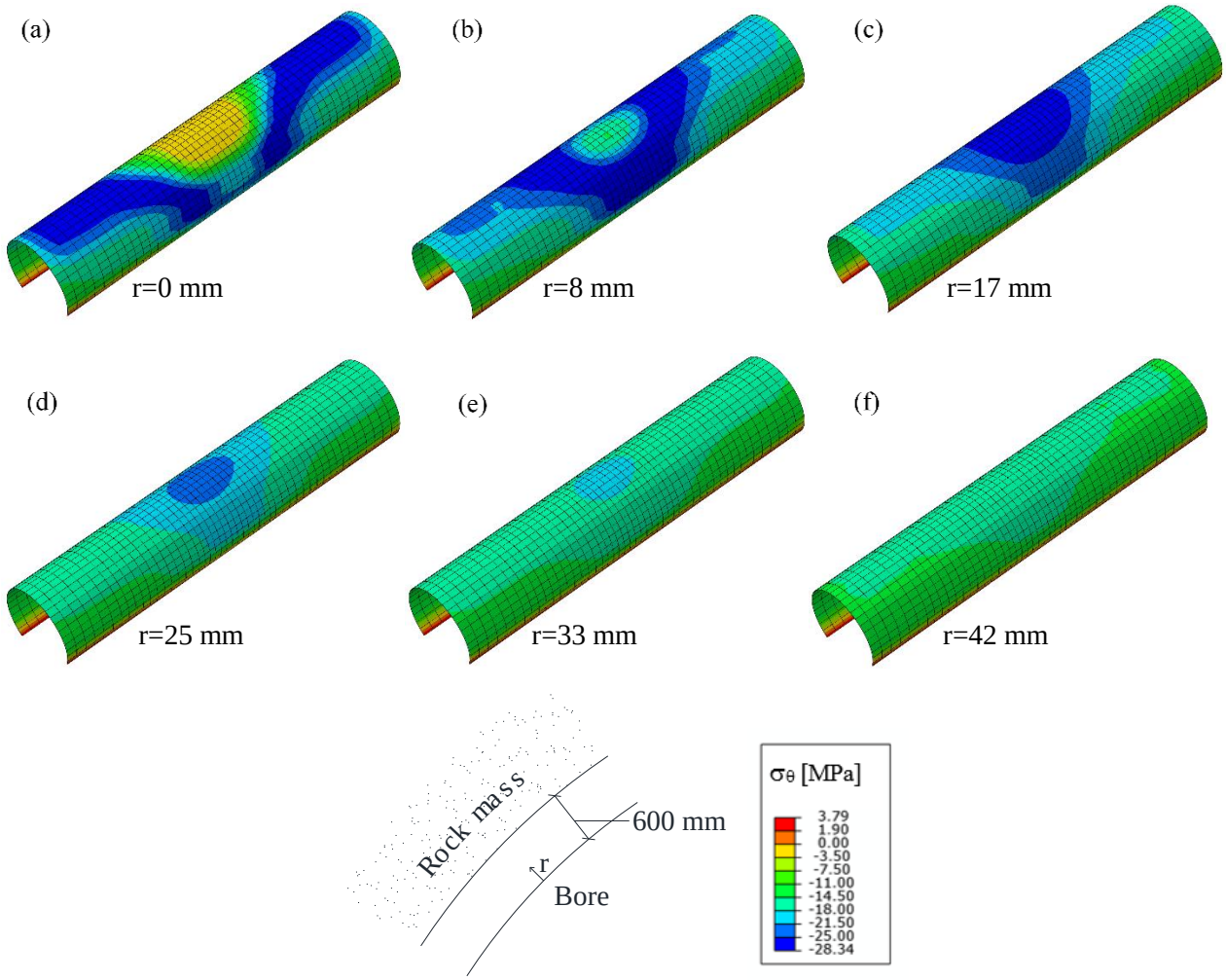

Figure 15 – Hoop stress after 910 sec within concrete lining at:

a) 0 mm (intrados surface); b) 8 mm; c) 17 mm; d) 25 mm; e) 33 mm f) 42 mm from lining intrados.

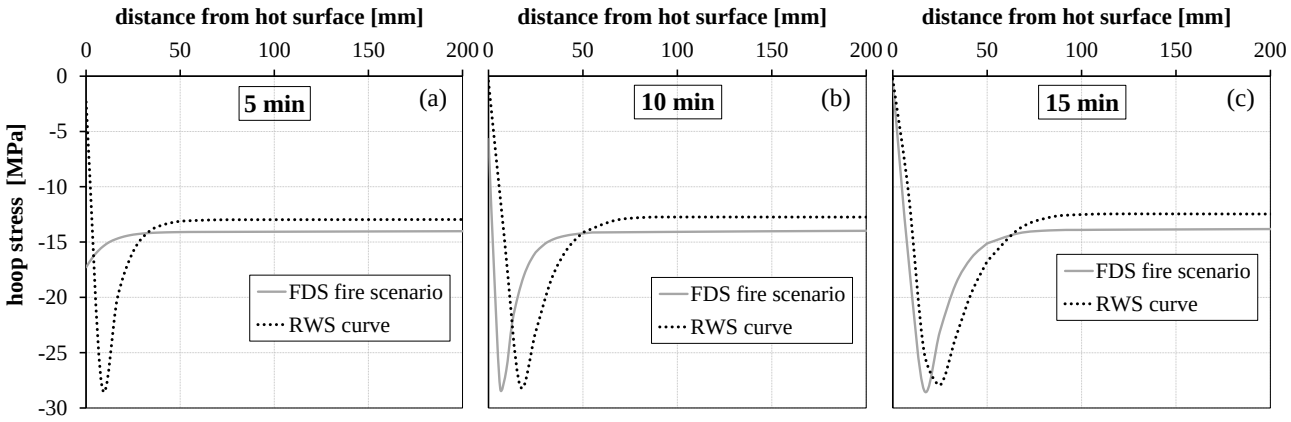

Figure 16 – Comparisons between mechanical results obtained by exploiting CFD fire modeling (with reference to the maximum heated point) and those obtained by uniformly applying the RWS curve after a) 5 min, b) 10 min, c) 15 min.

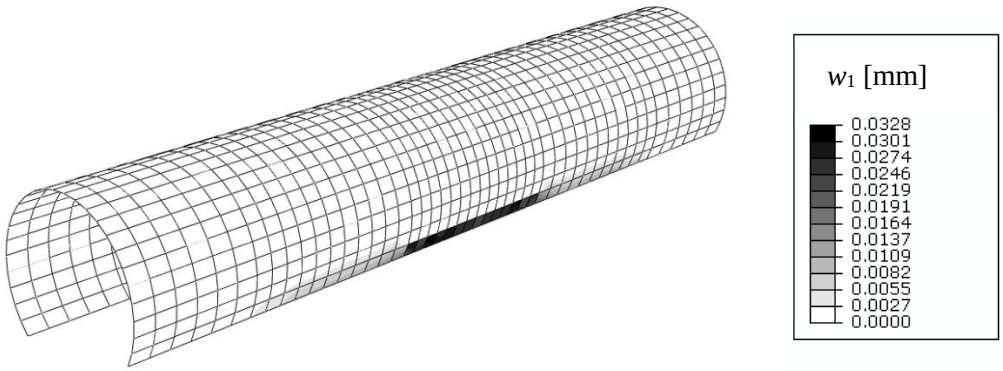

Figure 17 – Crack pattern in the concrete lining intrados after 910 sec and resulting crack width w_1.

From the performed non-linear structural analysis some information concerning crack pattern development can be also obtained. Crack distribution at the intrados of concrete lining relative to the time instant corresponding to the peak of RHR curve is reported in Figure 17. The presence of cracks in the bottom part of the lining benches, near the connection with paving, is mainly related to the discontinuity in lining geometry and material properties (both thermal and mechanical); their spotted distribution along the longitudinal direction can be explained by considering the heating and the equilibrium conditions in the lining. As can be observed from the temperature distribution across lining thickness reported in Figure 11, only a limited portion of the ceiling is actually subjected to high temperatures, while the surrounding region is characterized by much lower values. So, while the hotter portion tends to expand, the colder ones do not expand at the same manner, but rather oppose to this expansion by providing a confinement action. This leads to the appearance of higher tensile stresses in the lower part of the benches that exceed concrete tensile strength only in the tunnel region approximately corresponding to the position of the burning vehicle, thus leading to cracking appearance. On the contrary, when considering RWS curve – leading to a more severe but uniform temperature distribution than the actual fire scenario – crack formation does not take place in the lining, since tensile stresses appearing at benches remain lower than concrete tensile strength for all the fire exposure instants.

Based on the obtained results, for the considered case study, it seems that standard RWS fire curve can be safely used for the evaluation of thermal field and compressive hoop stresses within lining thickness. Even if RWS provides conservative results, the maximum values of temperatures and compressive hoop stresses are almost coincident with those obtained by applying a more refined CFD fire modeling, at least for the instants closer to maximum heating. Therefore, RWS might appear as a good compromise between effectiveness and simplicity.

However, its application does not allow to correctly catch the actual stress distribution in the lining (both in its thickness and along its transversal cross-section), and this can in turn affects cracking development, as shown in Figure 17. So, the use of a more realistic model of the fire seems crucial to understand correctly the behavior of tunnels subjected to fire and to control their possible weaknesses, such as the appearance of cracks.

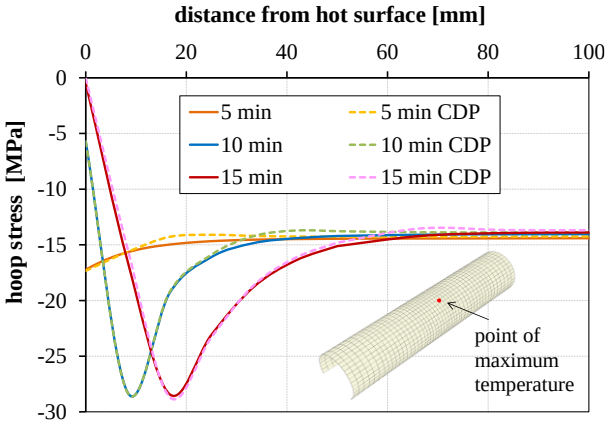

Figure 18 – Comparison between hoop stress distributions across concrete lining thickness obtained by considering "2D-PARC FIRE" and CDP model.

Finally, the use of 2D-PARC FIRE to simulate concrete behavior is compared with the well-known Concrete Damaged Plasticity model (CDP), available in ABAQUS library. As shown in Figure 18, the two models provide almost equal results for the considered case study, but in performing the analyses, 2D-PARC FIRE seems to be characterized by a greater numerical stability and the convergence seems less affected by the parameters needed for the definition of concrete behavior.

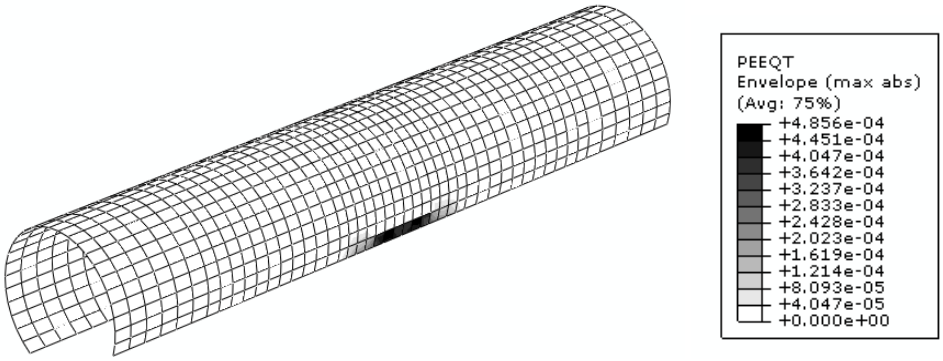

Figure 19 - Distributions of equivalent tensile plastic strain (PEEQT) in the concrete lining intrados after 910 sec.

Moreover, CDP model does not gives direct information on crack width, but it simply provides an indication of crack pattern, through the tensile equivalent plastic strain (PEEQT) distribution. However, by comparing Figure 17, relative to 2D-PARC FIRE crack pattern and Figure 19, relative to CDP tensile equivalent plastic strain distribution for the same fire duration, a close correspondence can be stated, thus further validating the use of 2D-PARC model for the description of the behavior of concrete lining subjected to fire.

5 Conclusions

This paper describes a multi-disciplinary procedure for the structural assessment of the fire safety of tunnel linings, based on the modeling of the three main features involved: fire dynamics (through CFD techniques), thermal behavior and structural response (through FE simulations). This work represents a first attempt to describe the actual behavior of concrete linings during a real fire and it wants to contribute to a better understanding of the structural response of these elements. In particular, the main goal of the outlined modeling strategy is to evaluate how a detailed fire simulation can affect the mechanical results, instead of applying standard fire curves as spatially uniform input data, as commonly done when the focus of the work is the structural performance. Based on the results discussed in this paper the following conclusions can be drawn:

- CFD simulation allows considering the real fire development, which gives rise to a three-dimensional heat spreading that influences the temperature and the fire-induced stress distribution

across the lining. Standard fire curves specifically conceived for tunnels, like RWS, can be however successfully applied for the evaluation of the temperature distribution in concrete lining, since they lay, as expected, on the safe side. On the contrary, their adoption may lead to a misinterpretation of structural performance, since the non-uniform temperature distribution, which is disregarded by standard approaches, may lead to an important confinement action that can in turn results in concrete cracking.

- The adoption of a refined non-linear model for concrete is mandatory for a realistic description of concrete behavior under fire load. Within this context, the possibility of correctly managing the occurrence of concrete cracking is very important. On this point, it can be observed that 2D-PARC FIRE model represents an interesting alternative to other constitutive models available in software libraries (as an example, the well-known concrete damaged plasticity in ABAQUS). It is indeed able to consider the most important mechanisms (i.e. aggregate bridging and interlock) that take place after crack formation and it is able to provide a numerical estimate of crack width, whose evaluation is of primary interest in unreinforced concrete tunnel design.

Aknowledgments

The contribution of M. Sc. Eng. Luca Zanichelli in data processing is gratefully acknowledged.

This research did not receive any specific grant from funding agencies in the public, commercial, or not-for-profit sectors.

References

[1] Kodur VKR, Naser MZ. Strategies for mitigating fire hazards in transportation infrastructure. In: Nigro E, Bilotta A, editors. 2nd Int. Fire Saf. Symp. (IFireSS 2017), Naples, Italy: 2017, p. 3–11.

[2] Carvel R. A review of tunnel fire research from Edinburgh. Fire Saf J 2016. https://doi.org/https://doi.org/10.1016/j.firesaf.2016.02.004.

[3] Feist C, Aschaber M, Hofstetter G. Numerical simulation of the load-carrying behavior of RC tunnel structures exposed to fire. Finite Elem Anal Des 2009;45:958–65. https://doi.org/10.1016/j.finel.2009.09.010.

[4] Mansour MH. Theoretical analysis of tunnel lining subjected to fire. J Engeneering Sci Assiut Univ 2010;38:619–40.

[5] Sýkora J, Jarušková D, Šejnoha M, Šejnoha J. Fire risk analysis focused on damage of the tunnel lining. Fire Saf J 2018;95:51–65. https://doi.org/10.1016/j.firesaf.2017.10.008.

[6] UNI EN 1992-1-2:2019. Eurocode 2 - Design of concrete structures - Part 1-2: General rules - Structural fire design. 2019.

[7] Maraveas C, Vrakas AA. Design of Concrete Tunnel Linings for Fire Safety. Struct Eng Int 2014;24:319–29. https://doi.org/10.2749/101686614X13830790993041.

[8] International Tunnelling Association (ITA). Guidelines for structural fire resistance for road tunnels. 2004.

[9] Li YZ, Ingason H. The maximum ceiling gas temperature in a large tunnel fire. Fire Saf J 2012;48:38–48. https://doi.org/10.1016/j.firesaf.2011.12.011.

[10] Glasa J, Valasek L. Study on Applicability of FDS+Evac for Evacuation Modeling in Case of Road Tunnel Fire. Res J Appl Sci Eng Technol 2014;7:3603–15. https://doi.org/10.19026/rjaset.7.713.

[11] Liang Q, Li Y, Li J, Xu H, Li K. Numerical studies on the smoke control by water mist screens with transverse ventilation in tunnel fires. Tunn Undergr Sp Technol 2017;64:177–83. https://doi.org/10.1016/j.tust.2017.01.017.

[12] Li YZ, Ingason H. Effect of cross section on critical velocity in longitudinally ventilated tunnel fires. Fire Saf J 2017;91:303–11. https://doi.org/https://doi.org/10.1016/j.firesaf.2017.03.069.

[13] Feenstra JA, Hofmeyer H, Van Herpen RAP, Mahendran M. Automated two-way coupling of CFD fire simulations to thermomechanical FE analyses at the overall structural level. Fire Saf J 2018;96:165–75. https://doi.org/10.1016/j.firesaf.2017.11.007.

[14] Zhang C, Silva JG, Weinschenk C, Kamikawa D, Hasemi Y. Simulation Methodology for Coupled Fire-Structure Analysis: Modeling Localized Fire Tests on a Steel Column. Fire Technol 2016;52:239–62. https://doi.org/10.1007/s10694-015-0495-9.

[15] Alos-Moya J, Paya-Zaforteza I, Garlock MEM, Loma-Ossorio E, Schiffner D, Hospitaler A. Analysis of a bridge failure due to fire using computational fluid dynamics and finite element models. Eng Struct 2014;68:96–110. https://doi.org/10.1016/j.engstruct.2014.02.022.

[16] Malendowski M, Glema A. Development and Implementation of Coupling Method for CFD-FEM Analyses of Steel Structures in Natural Fire. Procedia Eng 2017;172:692–700. https://doi.org/10.1016/j.proeng.2017.02.082.

[17] Zhang C, Yu HX, Choe L, Gross J, Li GH. Simulating the fire-thermal-structural behavior in a localized fire test on a bare steel beam. Eng Struct 2018;163:61–70. https://doi.org/10.1016/j.engstruct.2018.02.036.

[18] McGrattan K, Hostikka S, Floyd J, Baum HR, Rehm RG, Mell W, et al. Fire dynamics simulator (version 5), technical reference guide. vol. 1018. 2010.

[19] ABAQUS Documentation, Dassault Systèmes Simulia Corp., Providence, RI, USA 2018.

[20] Wickström U, Duthinh D, McGrattan KB. Adiabatic surface temperature for calculating heat transfer to fire exposed structures. Elev. Int. Interflam Conf., London: Interscience Communications; 2007.

[21] Malendowski M. Analytical Solution for Adiabatic Surface Temperature (AST). Fire Technol 2017;53:413–20. https://doi.org/10.1007/s10694-016-0585-3.

[22] Cheong MK, Cheong WO, Leong KW, Lemaire AD, Noordijk LM, Tarada F. Heat Release Rates of Heavy Goods Vehicle Fires in Tunnels. BHR Int Symp Aerodyn Vent Fire Tunnels 2013:10.

[23] Bernardi P, Cerioni R, Michelini E, Migliazza M. Numerical study on tunnel final lining behaviour. In: Kocsonya P, editor. Proc. ITA-AITES World Tunn. Congr. - Safe Tunn. City Environ., Budapest: 2009, p. 598-600 (extended abstract).

[24] AFTES. Plain concrete in tunnels. Tunnels Ouvrages Souterr 2000;158.

[25] Papanikolaou VK, Kappos AJ. Practical nonlinear analysis of unreinforced concrete tunnel linings. Tunn Undergr Sp Technol 2014;40:127–40. https://doi.org/10.1016/j.tust.2013.09.016.

[26] Franzen T, Garshol K., Tomisawa N. Sprayed concrete for final linings: ITA working group report. Tunn Undergr Sp Technol 2001;16:295–309. https://doi.org/10.1016/S0886-7798(01)00052-9.

[27] Cerioni R, Iori I, Michelini E, Bernardi P. Multi-directional modeling of crack pattern in 2D R/C members. Eng

Fract Mech 2008;75:615–28. https://doi.org/10.1016/j.engfracmech.2007.04.012.

[28] Bernardi P, Cerioni R, Michelini E. Numerical modelling of the behaviour of SFRC elements in presence of multiple cracks. Proceeding 8th RILEM Int. Symp. fibre Reinf. Concr. - Challenges Oppor., Guimarães (Portugal), September 19-21, Extended Abstract: 2012, p. 219–20, Full paper on CD Rom.

[29] Bernardi P, Cerioni R, Michelini E, Sirico A. Numerical modeling of the cracking behavior of RC and SFRC shear-critical beams. Eng Fract Mech 2016;167. https://doi.org/10.1016/j.engfracmech.2016.04.008.

[30] Bernardi P, Cerioni R, Michelini E, Sirico A. Transverse reinforcement optimization of a precast special roof element through an experimental and numerical procedure. Eng Struct 2020;203:109894. https://doi.org/10.1016/j.engstruct.2019.109894.

[31] Bernardi P, Cerioni R, Michelini E, Sirico A. Numerical study on concrete tunnel lining subjected to fire. Ital. Concr. Days Congr., Rome: 2016, p. on pen-drive.

[32] Sirico A. Development of a nonlinear model for RC/FRC elements applied to the analysis of tunnel linings under fire conditions. PhD Thesis, University of Parma, Department of Engineering and Architecture: 2017.

[33] Bažant ZP, Oh BH. Crack band theory for fracture of concrete. Matériaux Constr 1983;16:155–77. https://doi.org/10.1007/BF02486267.

[34] Aguado J V., Albero V, Espinos A, Hospitaler A, Romero ML. A 3D finite element model for predicting the fire behavior of hollow-core slabs. Eng Struct 2016;108:12–27. https://doi.org/10.1016/j.engstruct.2015.11.008.

[35] Gernay T, Franssen J-M. A comparison between explicit and implicit modelling of transient creep strain in concrete uniaxial constitutive relationships. Proc. Fire Mater. 2011 Conf., San Francisco: 2011, p. 405–16.

[36] Lu L, Yuan Y, Caspeele R, Taerwe L. Influencing factors for fire performance of simply supported RC beams with implicit and explicit transient creep strain material models. Fire Saf J 2015;73:29–36. https://doi.org/10.1016/j.firesaf.2015.02.009.

[37] Sadaoui A, Khennane A. Effect of transient creep on the behaviour of reinforced concrete columns in fire. Eng Struct 2009;31:2203–8. https://doi.org/10.1016/j.engstruct.2009.04.005.

[38] Lange D, Jansson R. A comparison of an explicit and an implicit transient strain formulation for concrete in fire. Fire Saf Sci – Proc 11th Int Symp 2014;11:572–83. https://doi.org/10.3801/IAFSS.FSS.11-572.

[39] EN 1992-1-1:2015. Eurocode 2 - Design of concrete structures - Part 1-1 : General rules and rules for buildings. 2015.

[40] Heskestad G. Fire Plumes, Flame Height, and Air Entrainment. SFPE Handb. Fire Prot. Eng., New York, NY: Springer New York; 2016, p. 396–428. https://doi.org/10.1007/978-1-4939-2565-0_13.

[41] Quintiere JG. Fundamentals of Enclosure Fire “Zone” Models. J Fire Prot Eng 1989;1:99–119.

https://doi.org/10.1177/104239158900100302.

[42] Cheong MK, Spearpoint MJ, Fleischmann CM. Calibrating an FDS simulation of goods-vehicle fire growth in a tunnel using the Runehamar experiment. J Fire Prot Eng 2009;19:177–96. https://doi.org/10.1177/1042391508101981.

[43] Galli G, Grimaldi A, Leonardi A. Three-dimensional modelling of tunnel excavation and lining. Comput Geotech 2004;31:171–83. https://doi.org/10.1016/j.compgeo.2004.02.003.

[44] Bernardi P, Cerioni R, Michelini E, Sirico A. NLFEA of tunnel linings under fire conditions. In: Nigro E, Bilotta A, editors. 2nd Int. Fire Saf. Symp. (IFireSS 2017), Naples, Italy: 2017, p. 719–26.

[45] Ariyanayagam AD, Mahendran M. Development of realistic design fire time-temperature curves for the testing of cold-formed steel wall systems. Front Struct Civ Eng 2014;8:427–47. https://doi.org/10.1007/s11709-014-0279-1.